Resonance Raman Spectra and Photophysical Properties of Ruthenium Complexes with the 3,3′- Bipyridazine Ligand

Joseph S. Gardner[†] and Dennis P. Strommen*

Department of Chemistry, Idaho State University, Pocatello, Idaho 83209

Witold S. Szulbinski,[‡] Haiquan Su, and James R. Kincaid*

Department of Chemistry, Marquette University, Milwaukee, Wisconsin 53201-1881

Received: June 14, 2002; In Final Form: November 13, 2002

This report documents the spectroscopic and photophysical properties of the complexes, $Ru(bpdz)_3^{2+}$ and $[Ru(bpy)_2(bpdz)]^{2+}$, where bpdz = 3,3′-bipyridazine and bpy = 2,2′-bipyridine. Specifically, the complexes were characterized by UV−visible, emission, resonance Raman (RR), and transient resonance Raman (TR^3) spectroscopic data, as well as lifetime measurements. The RR spectrum of the $Ru(bpdz)_3^{2+}$ complex documents the characteristic modes of the coordinated ligand, whereas the RR spectra of the heteroleptic complex, $[Ru(bpy)_2(bpdz)]^{2+}$, obtained at judiciously chosen excitation wavelengths, reveal selective enhancement of either bpy modes or bpdz modes, depending upon the particular excitation wavelength, permitting definitive assignment of the observed electronic absorption bands and establishing the lowest energy electronic transition as having a Ru-to-bpdz charge-transfer character. The TR^3 spectrum of the $Ru(bpdz)_3^{2+}$ complex reveals the characteristic frequencies of the coordinated $bpdz^{-\bullet}$ anion radical, as expected, whereas corresponding studies of the heteroleptic complex, $[Ru(bpy)_2(bpdz)]^{2+}$, reveal these characteristic $bpdz^{-\bullet}$ modes in the absence of any modes attributable to $bpy^{-\bullet}$ anion radicals, providing definitive evidence for the $[Ru(III)(bpy)_2(bpdz^{-\bullet})]^{2+}$ formulation of the excited state of this complex. Lifetime measurements for both complexes, made over a wide range of temperatures and interpreted with a model derived from previous measurements made on a large number of similar complexes, indicate that the two complexes of interest decay by different nonradiative pathways resulting from thermal population of a ligand field ^{3}dd and/or a lower lying 4th ^{3}MLCT state.

Introduction

Complexes of ruthenium(II) with 2,2′-bipyridine(bpy) and related ligands continue to attract much attention as potential components of practical solar energy conversion devices[1−5] and as a set of synthetically versatile, well-behaved systems to investigate the fundamental principles of radiative and nonradiative decay of long-lived metal-to-ligand charge-transfer (^{3}MLCT) excited states. The electronic structure and reactivity of these excited states are naturally dependent upon the precise chemical nature of the constituent ligand,[6] and detailed spectroscopic studies of such species can provide important insights into these issues.

Resonance Raman (RR) spectroscopy has proven to be a useful tool in investigating ground and excited-state properties of complexes in this family.[7−10] Selective enhancement of vibrational modes coupled to allowed charge transfer electronic transitions provides the frequencies and intensities of a selected group of (generally) totally symmetric vibrations for the ground state. In addition, the degree of enhancement for individual bands provides some indication of the distortions, which favor the excited-state geometry, providing the character of the normal modes is known. As was first demonstrated by Dallinger and co-workers, time-resolved resonance Raman (TR^3) spectroscopy serves as an especially effective probe of these relatively long-lived ^{3}MLCT states.[8] In fact, subsequent studies by our group[7] and others[9,10] illustrated the utility of TR^3 methods to document selective population of individual ligand-localized excited states for various heteroleptic complexes. Most recently, this approach was applied to complexes containing inherently asymmetric ligands, such as pyridylpyrazine, to reveal charge polarization within the individual ligand-localized state,[11,12] clearly demonstrating the exquisite sensitivity of the technique to subtle alterations in molecular and electronic structure.

Although considerable attention has been focused on 2,2′-bipyridine (bpy) and derivatives bearing various peripheral substituents,[6,13] the so-called diazine ligands (shown in Figure 1), bearing two ring N-heteroatoms, are of special interest in that not only do they represent chelating ligands whose LUMOs are substantially lower in energy than many of the substituted bipyridines, but they also have been shown to be useful synthetic templates in the construction of zeolite-based organized molecular assemblies.[14]

Although previous studies have documented the spectroscopic and photophysical properties of the homoleptic and heteroleptic divalent ruthenium complexes involving several of these ligands, until now, little attention has been given to the complexes bearing the bpdz ligand. In the present work, RR and TR^3 methods are employed to characterize the molecular and electronic structure of the ground and lowest ^{3}MLCT states of the tris-homoleptic and heteroleptic complexes, $Ru(bpdz)_3^{2+}$ and $Ru(bpy)_2(bpdz)^{2+}$, and temperature-dependent lifetime measurements are made to define the important nonradiative decay pathways available to the two complexes.

* To whom correspondence should be addressed.

[†] Present Address: Department of Chemistry, Brigham Young University, Provo Utah.

[‡] Present address: Central Mining Institute, 40-166 Katowice, Poland.

10.1021/jp0214312 CCC: $25.00
Published on Web 12/28/2002

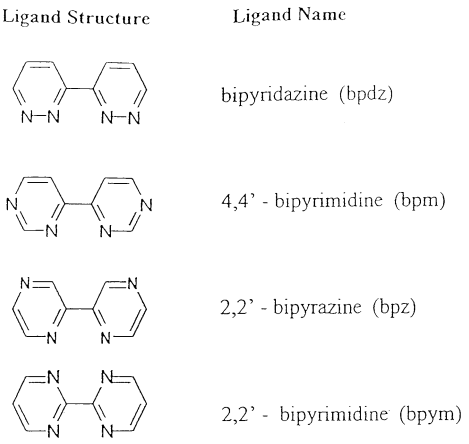

Figure 1. Structures of the α-diazines.

Experimental Section

1. Materials. Palladium, 5% on carbon catalyst, was obtained from Avocado Research Chemicals Ltd. Pyridazine (98% purity) was obtained from Aldrich Chemicals Co.,and $RuCl_3 \cdot 3H_2O$ (99.9% purity; Ru = 40.24%) and $Ru(NH_3)_6Cl_3$ (99.9% purity; Ru = 32.7%) from Alfa AESAR chemicals.

2. Preparation of Compounds. *2.1. Synthesis of 3,3′ Bipyridazine (bpdz).* Using previous methods,[15] a mixture of 5 g of pyridazine and 0.5 g of 5% palladium on carbon was stirred and refluxed for 3−4 days. Then this mixture was cooled, diluted with 15 mL of chloroform, and filtered using a filter agent to separate the fine catalyst. This was followed by two washings of the spent catalyst with additional 15 mL portions of chloroform. The filtrate and washings were combined, and the chloroform was removed under nitrogen. Purification methods that were used differed slightly from the literature procedures. Our methods consisted of crystallization from water followed by two sublimations at 125−130 °C.

2.2. Synthesis of Tris(3,3′-bipyridazine) Ru(II)chloride, $[Ru(bpdz)_3]Cl_2$. A ratio of 3.5 to 1 of 3,3′-bipyridazine to $Ru(DMSO)_4Cl_2$ was used in forming this complex. $Ru(DMSO)_4Cl_2$ was obtained from a preparation as described in previous literature.[16] A 30 mg [∼0.18 mmol] sample of 3,3′-bipyridazine was placed in a reflux flask with 27.8 mg [0.051 mmol] of $Ru(DMSO)_4Cl_2$ and approximately 2.5 mL of H_2O. This solution was refluxed for 24 h yielding a dark red product. Purification of the product was achieved by chromatography on a column of Lipophilic Sephadex LH-20 using 50% ethanol as the eluent.

2.3. $[Ru(bpy)_2(bpdz)]Cl_2$ Prepared from $[Ru(bpy)_2]Cl_2$. $[Ru(bpy)_2]Cl_2$ was prepared previously in our laboratory according to methods described in earlier publications.[14] $[Ru(bpy)_2(bpdz)]Cl_2$ was synthesized following literature methods.[14] The bpdz ligand (15 mg) [0.10 mmol] was added to 30 mg [0.062 mmol] of $[Ru(bpy)_2]Cl_2$ in 1 mL of ethylene glycol. This solution was brought to reflux under Argon gas and stirred for 30 min. At reflux, the dark purple solution quickly turns red in color. This solution was cooled in an ice bath, and a saturated aqueous solution of NH_4PF_6 was added slowly to induce precipitation of $[Ru(bpy)_2(bpdz)](PF_6)_2 \cdot H_2O$. This black precipitate was collected via vacuum filtration and washed with 2 mL of R.O. water. The PF_6^- salt of the heteroleptic species was purified by chromatography on a column of alumina using acetonitrile as the eluent. The chloride form of the heteroleptic species was subsequently obtained by ion exchange.

3. Spectroscopic Measurements. *3.1. UV−Vis, Emission, and FT-IR Spectra.* A Shimadzu UV-2101 PC scanning spectrophotometer was used to take UV−vis measurements at room temperature. Fluorescence spectra were obtained from a Perkin-Elmer luminescence spectrophotometer model LS50B. Infrared spectra were measured using a Perkin-Elmer 16PC FT-IR and a Mattson Galaxy Series FTIR 3000.

3.2. Resonance Raman (RR) and Transient Resonance Raman (TR^3) Spectra. The RR spectra acquired at Idaho State University employed a Spex model 1404 double monochromator equipped with a thermoelectrically cooled Hamamatsu R928P photomultiplier tube and a model 1459 illumination/collection system (90 degree collection geometry). The excitation lines at 514.5 and 457.9 nm were provided by a Coherent model 70A Argon ion laser.

At Marquette University, RR and TR^3 spectra were acquired using a Spex model 1269 spectrometer equipped with a Princeton Instruments ICCD-576 UV-enhanced detector, FG-100 pulse generator, and 356 or 413 nm notch filters (Kaiser Optical Systems, Ann Arbor, MI); a Spex model 1877 spectrometer equipped with a Tracor Northern rapid scan spectrometer, model TN-6500, and diode array detector, model TN-6100, or a conventional Raman spectrometer (Spex model 1403 double monochromator equipped with a Spex model DM1B controller and a Hamamatsu R928 PMT). The excitation sources used were the 350.9, 406.7, and 413.1 nm laser lines from a Coherent model Innova 100-K3 Kr^+ ion laser, the 441.5 nm laser line from a Liconix He−Cd laser, or the 457.9 and 488.0 nm laser lines from a Spectra-Physics Ar^+ ion laser, model 2025-05. For the transient measurements the 3rd harmonic of a Spectra Physics DCR-3A Nd:YAG laser was used to provide 354.7 nm radiation. Average power at the laser ranged from 125 to 175 mW at a repetition rate of 20 Hz. The average pulse width in these experiments was 10 ns. All Raman spectra of the free ruthenium complex in water were obtained in rotating NMR tubes (5 mm i.d.) to avoid localized heating by the laser beam. The scattered light was collected with 135° backscattering geometry and a conventional two-lens collection system. Before the measurements, the liquid samples (prepared in DI water, or propylene carbonate, PC) were degassed by triple freeze−pump−thaw, directly in the NMR tubes, and then sealed.

3.3. Emission Spectra. The spectroscopic apparatus was the same as for the Raman measurements (Spex model 1403). The laser excitation was focused onto spun NMR tubes containing the samples, with the laser power of 10−20 mW at the sample. Spectra were recorded with 40 cm^{-1} increments.

3.4. Lifetime Measurements. The samples for the measurements were degassed as described before. The third harmonic (354.7 nm; 10−15 ns pulse-width) of a Quanta-Ray (Spectra-Physics) model GCR-11 or DCR-3 Nd:YAG laser (operated at 20 Hz frequency) was used as the excitation source (the power at the sample was in all cases below 0.05 mJ/pulse). The light emitted from the sample in the spinning NMR tube was transferred through glass collecting and transferring lenses and a 580 nm cutoff filter to a Spex 340S spectrometer equipped with an RCAC31034A-02 PMT with an applied voltage of 1800 V. The PMT output signal was directed to a LeCroy 9450A Dual 300 MHz oscilloscope. The emission was monitored at an appropriately chosen wavelength (at 622 nm for $Ru(bpdz)_3^{2+}$ and 703 nm for $Ru(bpy)_2(bpdz)^{2+}$). In all cases, 3000 scans of the emission decay curve were averaged and transferred to the computer. The curves were then fitted by a monoexponential model using facilities of the commercial software (PSI−Plot) based on the Marquardt−Levenberg algorithm.

For the temperature dependent lifetime measurements, the samples were placed into a double wall Dewar cell of in-house

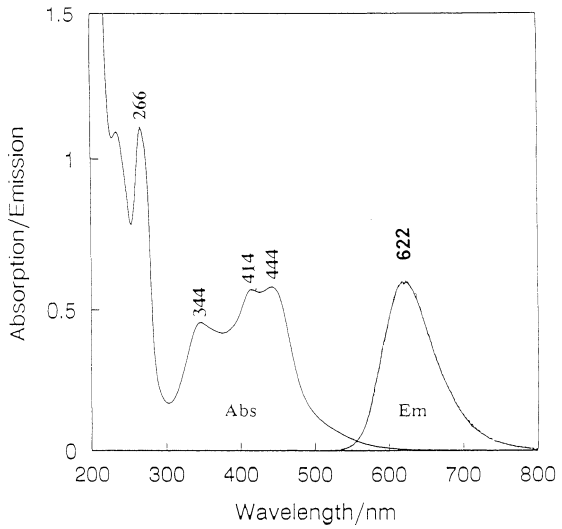

Figure 2. Absorption and emission spectra of $Ru(bpdz)_3^{2+}$.

design. Prior to the measurement, the samples were thoroughly degassed by bubbling Ar through the solution (for polycarbonate solutions of $[Ru(bpdz)_3](PF_6)_2$, $[Ru(bpy)_2(bpdz)](PF_6)_2$, and $[Ru(bpy)_3](PF_6)_2$ the complexes were used with a concentration <10−5 M). During the experiments, the PC solution was continuously stirred by a magnetic stirrer to prevent local overheating and possible decomposition of the compounds. The temperature of the sample was measured (with 0.1 °C accuracy) using a thermocouple inserted into the sample or placed, as close as possible, to the spinning tube with sample immersed in the cooling (heating) bath. For the low-temperature measurements, the samples were cooled by EtOH/liquid nitrogen mixture (−60 °C) and then allowed to slowly warm to room temperature. During this period of time (3−4 h), the lifetime measurements were acquired every 3−4 °C change in temperature. The temperature variation during the collection of the data (500 sweeps per 25 s) was approximately 0.3−0.5 °C. The measurements at temperatures above 20 °C were taken with the same setup using boiling water as the heating fluid, while allowing it to slowly cool to room temperature.

Results and Discussion

A. Electronic Absorption and Emission Data. The absorption and emission spectra of an aqueous solution of the $[Ru(bpdz)_3]Cl_2$ complex are shown in Figure 2. The UV−visible spectrum consists of four bands centered at λ_{max} = 444, 414, 344, and 266 nm: the two electronic absorption bands centered at λ_{max} = 344 and 444 nm are assigned to MLCT transitions, the maximum at 414 nm is a vibrational sideband to the 444 nm peak, whereas the band at λ_{max} = 266 nm is due to a ligand-centered $\pi \rightarrow \pi^*$ transition.

As shown in Figure 3, for $[Ru(bpy)_2(bpdz)]Cl_2$, the visible absorption bands shown with a dotted line appear at λ_{max} = 410 and 472 nm. These bands in the visible region of the spectrum can be assigned to electronic transitions between $d(t_{2g})$ orbitals of the metal and the π^* orbitals of the bpy and bpdz ligands.[17] Inasmuch as the bpdz π^* orbital is lower in energy than that of the bpy counterpart,[13] it is expected that the absorption band maximizing at 472 nm is ascribable to the Ru → bpdz transition, whereas the higher energy band centered at 410 nm is associated with the Ru → bpy transition.

This can be rationalized by inspection of the qualitative energy diagram depicted in Figure 4, whose predictions are also entirely consistent with the RR data obtained in the present work, vide infra.

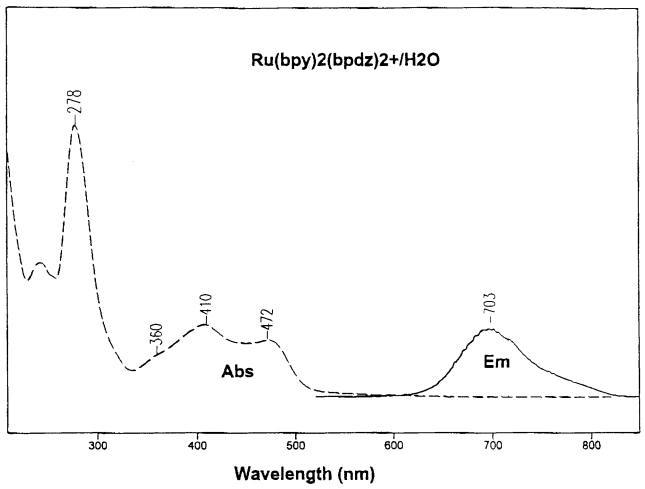

Figure 3. Absorption and emission spectra of $Ru(bpy)_2(bpdz)^{2+}$.

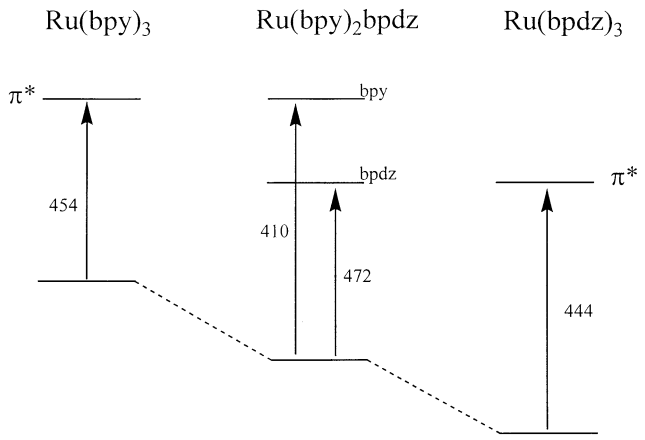

Figure 4. Qualitative energy level diagram showing expected changes for the heteroleptic complex.

The emission spectrum of the aqueous solution of the $[Ru(bpy)_2(bpdz)]Cl_2$ complex, obtained with 458 nm excitation, revealed phosphorescence at λ_{em} = 703 nm, as shown in Figure 3. This emission is 81 nm red-shifted with respect to that of the $[Ru(bpdz)_3]Cl_2$ complex (see Figure 2), a shift which is similar to that observed in the electronic absorption spectra, i.e., 472−444 nm (=1291 cm^{-1}) vs 702−622 nm (=1832 cm^{-1}). This shift is attributable to the donor strength of the bpdz, which, being greater than that of the bpy ligand,[13] raises the energy of the metal d orbitals in the heteroleptic complex, consequently lowering the energy of both the ^{1}MLCT absorption and ^{3}MLCT emission bands that are associated with the bpdz π^* orbital.

B. Resonance Raman and TR^3 data. *1. RR Spectra of the Ground-State Species. a. Resonance Enhancement Profiles.* Shown in Figure 5 are RR spectra of the homoleptic, tris-bpdz complex obtained at two excitation wavelengths, both of which exhibit the same set of modes and comparable intensities. These are the characteristic totally symmetric modes of the coordinated bpdz ligand, reported here for the first time. Additional modes at 786, 672, 372, and 342 cm^{-1} observed in the lower frequency region are not shown. The observed bands are consistent with those reported in an earlier work dealing with the RR and TR^3 spectra of bipyrazine complexes.[18]

In the case of the heteroleptic complex, $Ru(bpy)_2(bpdz)^{2+}$, it is expected that modes associated with both types of constituent ligands (i.e., bpy and bpdz) would exhibit resonance enhancement, depending on the proximity of the laser excitation line to a resonant metal-to-ligand charge-transfer electronic transition

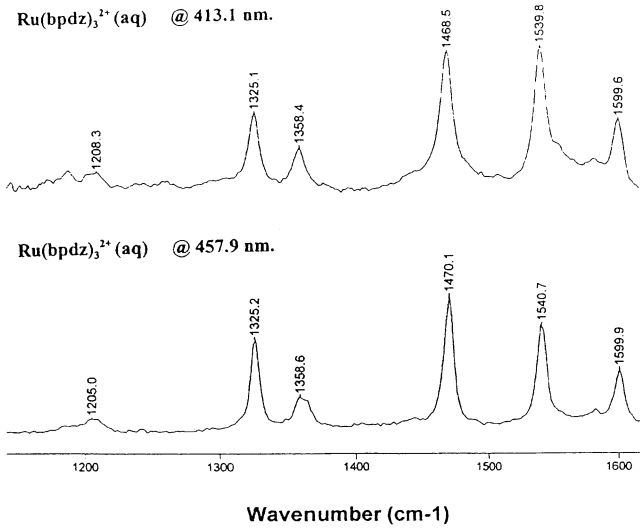

Figure 5. Resonance Raman spectra of $[Ru(bpdz)_3]Cl_2$. A. $\lambda_{ex} = 413.1$ nm. B. $\lambda_{ex} = 457.9$ nm.

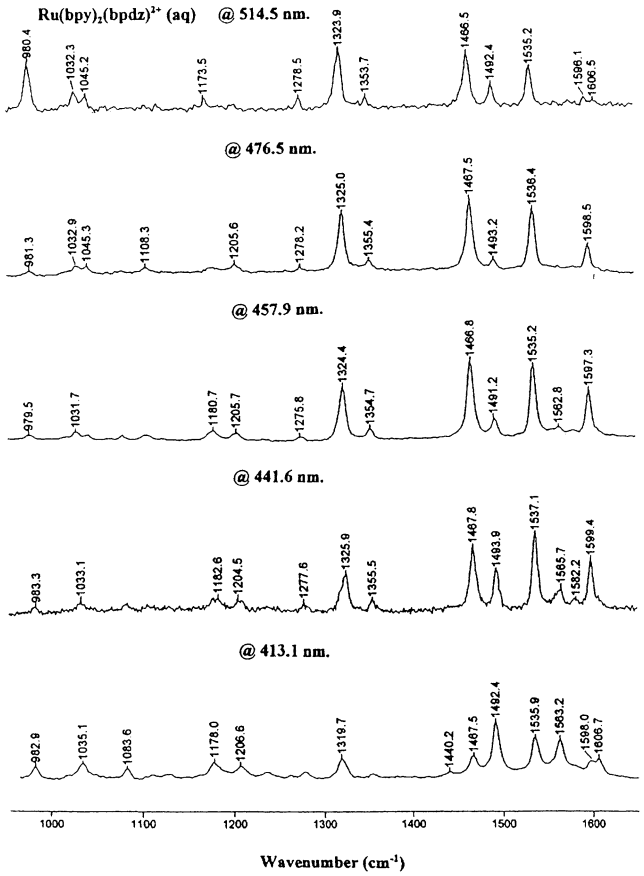

Figure 6. Resonance Raman spectra of $[Ru(bpy)_2(bpdz)]Cl_2$. The band at $\nu = 981$ cm^{-1} comes from the K_2SO_4 internal standard (0.1 M).

associated with a particular ligand, i.e., either bpy or bpdz. The RR spectra of the heteroleptic complex, acquired at several different excitation wavelengths, are depicted in Figure 6, with the modes attributable to coordinated bpy, based on extensive earlier studies.[7]

The four excitation wavelengths used to acquire these data span the entire absorption envelope of the heteroleptic complex (see Figure 3). Considering the intensities of the bands relative to the intensity of the nonresonance enhanced mode of the internal standard, sulfate ion (983 cm^{-1}), the following behavior is observed. With excitation at 476.5 nm, a wavelength nearly coincident with the maximum of the low energy electronic transition of the complex (see Figure 3), modes associated with the coordinated bpdz ligand are selectively enhanced; that is, the RR spectrum at this wavelength closely resembles those shown in Figure 4, with the only notable difference being the observed weak enhancement of the bpy mode at 1493 cm^{-1}. Such behavior provides convincing evidence for assignment of this lower energy electronic transition to that associated with the bpdz-localized ^{1}MLCT state. However, although there is a general increase in the intensities of bpy-associated modes in the spectra acquired with progressively higher energy excitations (i.e., 457.9 through 413.1 nm), it is clear that several of the bpdz-associated modes are also enhanced with these excitation lines. This behavior differs from that observed with other heteroleptic complexes studied earlier, such as those with 2,2′-bipyrazine, bpz, (i.e., $[Ru(bpy)_2(bpz)^{2+}]$, where only residual intensities of bpz modes are detectable in resonance with a Ru-bpy ^{1}MLCT transition near 400 nm.[7,11]

The most reasonable interpretation of the behavior observed here is that the absorption envelope centered near 413 nm in the spectrum of the heteroleptic complex is a superposition of ^{1}MLCT transitions to both the bpy and the bpdz ligands. This interpretation is consistent with the fact that, compared to other tris-homoleptic complexes that have been studied,[18] $Ru(bpdz)_3^{2+}$ exhibits an additional, relatively strong, electronic absorption band near 344 nm along with the typical absorption envelope appearing between 440 and 460 nm. We suspect that this is another ^{1}MLCT Ru → bpdz transition. Thus, considering the fact that the lower energy transition shifts from about 444 to 472 nm (i.e., approximately 1300 cm^{-1}) upon comparing the homoleptic and heteroleptic complexes, it is expected that the higher energy transition would experience a comparable shift, occurring somewhere near 360 nm for the latter. In fact, careful inspection of the absorption spectrum depicted in Figure 3 reveals a weak shoulder on the high energy side of the band centered near 410 nm. To the extent that this interpretation is valid, it provides a clear demonstration of the unique potential of the RR technique for establishing definitive assignments of complex electronic absorption profiles.

b. Frequency Shifts. Although the modes of a given ligand (bpy or bpdz) are observed near their characteristic frequencies, it is to be noted that tell-tale shifts consistent with the identity of the "spectator" ligands are indeed observed. For example, the frequencies of certain bpdz modes, such as those observed at 1541 and 1470 cm^{-1} shift to lower frequencies, by several wavenumbers, in the spectrum of the heteroleptic complex, compared to their values in the homoleptic complex, i.e., they occur at 1536 and 1467 cm^{-1}. This behavior is consistent with the fact that the bpy ligand is a stronger σ donor than the bpdz ligand; that is, the presence of the two bpy spectator ligands in the homoleptic complex leads to greater metal(dπ)−bpdz back-bonding and a slight lowering of the frequencies of the coordinated bpdz ligand. Thus, the RR technique is entirely capable of revealing very subtle changes in the electronic structure of these types of complexes.

2. TR^3 Spectra of the Lowest Energy ^{3}MLCT States. a. Homoleptic Complex. Shown in Figure 7 is the TR^3 spectrum of the $Ru(bpdz)_3^{2+}$ complex acquired with 354.7 nm excitation pulses (10−15 ns), conditions typically used to obtain the RR spectra of the lowest energy ^{3}MLCT states of such species,[8,11] along with the RR spectrum of the ground-state acquired with 350.9 nm cw excitation. In the top trace, the spectrum of the

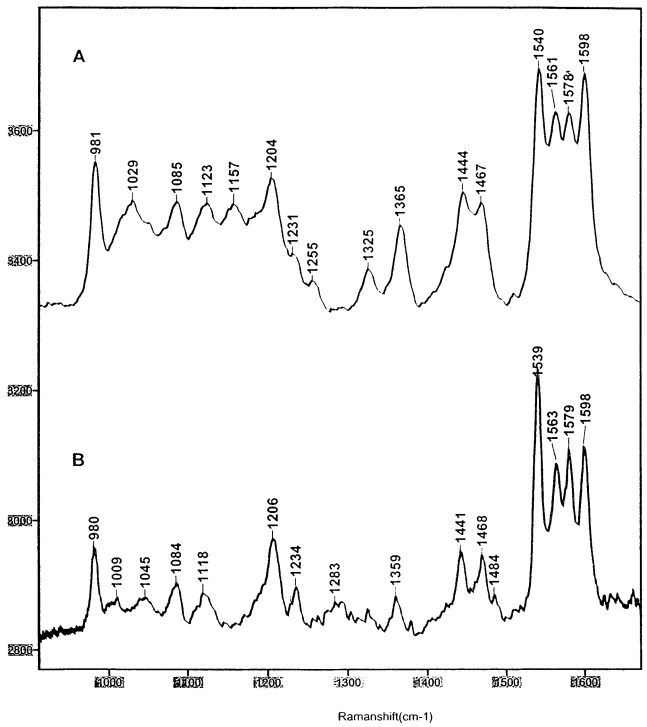

Figure 7. TR^3 and RR spectra of $[Ru(bpdz)_3]Cl_2$. A. TR^3 spectrum. B. Ground-state resonance Raman.

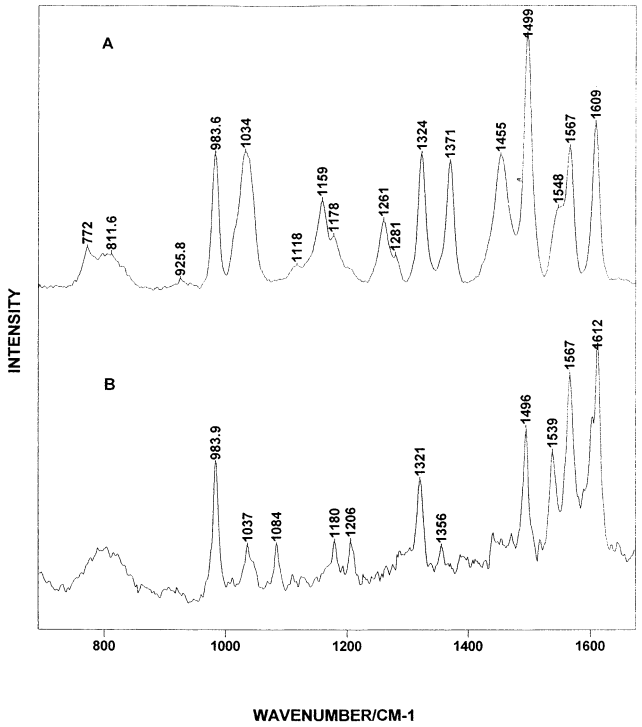

Figure 8. TR^3 and RR spectra of $[Ru(bpy)_2(bpdz)]Cl_2$. A. $\lambda_{ex} = 354.7$ nm. B. $\lambda_{ex} = 350.9$ nm.

^{3}MLCT excited state exhibits a new set of bands, in addition to those seen in the bottom trace.

This behavior is entirely consistent with that observed in similar studies of many other complexes of this type[8,11] and is attributable to RR enhancement of modes associated with the coordinated "neutral" bpdz ligands, as well as those of the coordinated anion radical ligand, $bpdz^{-\bullet}$; that is, the ^{3}MLCT is properly formulated as $[Ru(III)(bpdz)_2(bpdz^{-\bullet})]^{2+}$. In the top trace, the modes seen at 1029, 1157, 1257, 1325, 1365, and 1444 cm^{-1} may clearly be assigned to modes of the coordinated bpdz moiety because they do not appear in the cw spectrum. The residual bands originate from the neutral ligand species of the complex. We were unable to obtain a higher degree of saturation without sample degradation.

b. Heteroleptic Complex. The corresponding TR^3 and near-UV excited ground-state spectra of the $Ru(bpy)_2(bpdz)^{2+}$ complex are shown in Figure 8.

The most important observation to be noted is that the bands characteristic of a coordinated $bpy^{-\bullet}$ anion radical, whose frequencies have been well documented in many studies,[8,11] do not appear in the TR^3 spectrum shown in the top trace, whereas several of the bands attributable to the $bpdz^{-\bullet}$, observed in the top trace of Figure 7, are also observed here. For example, bands appear at 1159, 1271, 1371, and 1455 cm^{-1}, all of which have counterparts in the TR^3 of the $[Ru(bpdz)_3]^{2+}$. The 1029 cm^{-1} excited-state mode which is observed in the spectrum of the homoleptic complex is obscured by the 1037 cm^{-1} of the bpy but still can be discerned by comparison of the envelope in that region compared to the internal standard. It is noted that the frequencies are 2−6 cm^{-1} higher in this case which is also attributed to the presence of the bpy ligand.

C. Lifetime Measurements. Emission decay profiles, acquired at 295 K with the 354.7 nm excitation and a 10−15 ns pulse duration, for diluted (10^{-5} M) propylene carbonate (PC) solutions of the $[Ru(bpdz)_3](PF_6)_2$ complex ($\lambda_{em} = 622$ nm) and the $[Ru(bpy)_2(bpdz)](PF_6)_2$ complex ($\lambda_{em} = 703$ nm) exhibit mono- exponential behavior, yielding measured lifetimes (τ) of 980 and 220 ns, respectively. In aqueous solution, at 295 K, the lifetime of the tris-homoleptic complex, $[Ru(bpdz)_3]Cl_2$, is 535 ns, but attempts to determine the lifetime of the heteroleptic complex were unsuccessful because of the lower limit of our experimental measurement ability and are thus assumed to be less than 50 ns.

As has been shown in an elegant series of papers by Meyer and co-workers,[17] nonradiative decay of the ^{3}MLCT states of these types of complexes is most often dominated by thermal population of a largely triplet "ligand field" (LF) or "^{3}dd" state, but for some complexes, the energy gap (Δ_{LF}) between the ^{3}MLCT and the LF state is large, in which case the temperature dependence of the lifetime is dominated by contributions from a so-called "4th ^{3}MLCT" state which lies relatively close to the lowest lying manifold of ^{3}MLCT states. The relative importance of these two deactivation pathways and the kinetic parameters associated with each can best be evaluated by acquisition and analysis of lifetime data over a wide range of temperatures. Results of such studies for a number of such complexes[14,19] reveal varying behavior; that is, some complexes with relatively low energy LF states decay mainly through thermal population of the LF state, whereas those possessing high energy LF states exhibit parameters characteristic of decay through the "4th ^{3}MLCT" state. In fact, the temperature dependence of the lifetimes of certain complexes (i.e., those possessing LF states of intermediate energy) cannot be adequately modeled without invoking both thermally activated pathways.

Shown in Figure 9 are plots of the lifetimes acquired for each of the complexes as a function of temperature, with the results for the paradigmatic $Ru(bpy)_3^{2+}$ complex being included as a reference for comparison with data previously reported.[14,19]

Inasmuch as the detailed procedures and assumptions involved in the analysis of such data sets are fully explained elsewhere,[14c] it is only important here to summarize the derived kinetic parameters for each of the complexes, with their values being

TABLE 1: Kinetic Parameters for Selected Ru^{2+} Polypyridine Complexes Obtained from Temperature-Dependent Lifetime Measurements in PC Solution

complex	k_0 [s^{-1}]	k_{4th} [s^{-1}]	E_{4th} [cm^{-1}]	k_{LF} [s^{-1}]	E_{LF} [cm^{-1}]	ref
$Ru(bpdz)_3^{2+}$	6.84×10^5	1.03×10^8	1157	1.01×10^{13}	4361	this work
$Ru(bpy)_2(bpdz)^{2+}$	2.58×10^6	1.04×10^8	812			this work
$Ru(bpy)_3^{2+}$	6.1×10^5			4.0×10^{12}	3275	17
$Ru(bpy)_2(bpz)^{2+}$	2.1×10^6	3×10^7	800			14 and 19
$Ru(bpz)_2(bpy)^{2+}$	6.4×10^5	8×10^6	736	9×10^{13}	4632	19d
$Ru(bpz)_3^{2+}$	3.4×10^5			1.4×10^{14}	3902	14 and 19

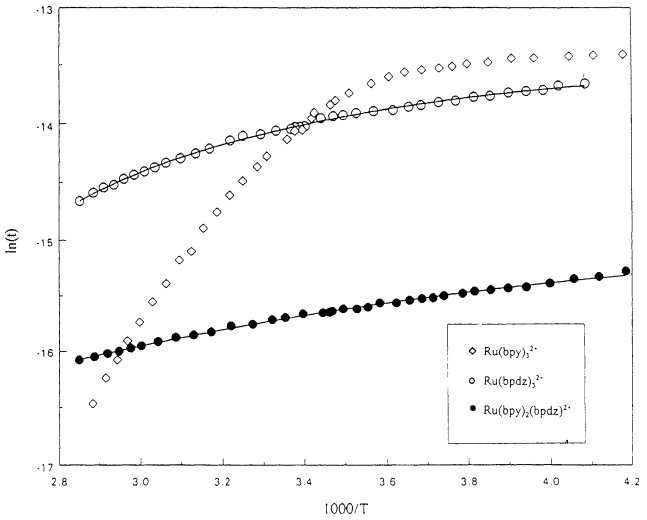

Figure 9. Temperature-dependent lifetime data obtained for $[Ru(bpy)_2(bpdz)](PF_6)_2$ (●, filled circles), $[Ru(bpdz)_3](PF_6)_2$ (○, open circles), and $[Ru(bpy)_3](PF_6)_2$ (□, squares) dissolved in PC (10^{-5}M). The solid line represents mono- or biexponential fit obtained using the following expression: $1/\tau_T = k_0 + k_{LF} \exp(-\Delta E_{LF}/k_bT) + k_{4th} \exp(-\Delta E_{4th}/k_bT)$.

given in Table 1, where the parameters are related by the following expression:

$$1/\tau_T = k_0 + k_{LF} \exp(-\Delta E_{LF}/k_bT) + k_{4th} \exp(-\Delta E_{4th}/k_bT) \quad (1)$$

where τ_T is the lifetime at temperature T; k_0 is $k_r + k_{nr}$ radiative and nonradiative decay rate constants; k_{4th} is the preexponential factor corresponding to the thermal population rate constant of the so-called "4th ^{3}MLCT" electronic excited state; E_{4th} is the energy gap between the ^{3}MLCT and 4th ^{3}MLCT electronic excited states; k_{LF} is the preexponential factor corresponding to the thermal population rate constant of the LF excited state; E_{LF} is the energy gap between ^{3}MLCT and LF electronic excited states.

Consideration of the values of the derived parameters reveals the following information. As has been shown previously,[14,17,19] the $Ru(bpy)_3^{2+}$ reference complex decays mainly through the relatively low-lying LF state, with its characteristic preexponential factor of $\sim 10^{12}-10^{13}$ s^{-1}, whereas the heteroleptic complex, $Ru(bpy)_2(bpdz)^{2+}$, apparently possesses an inaccessibly high energy LF state, the only accessible thermally activated pathway being that associated with the "4th ^{3}MLCT" state, with its corresponding preexponential factor having a characteristic value of $\sim 10^8$. The behavior of the homoleptic complex, $Ru(bpdz)_3^{2+}$, resembles that observed for certain other complexes previously studied[14,19] (e.g., the last entry in Table 1), where a satisfactory fit of the experimental data points can be obtained only by including both thermally activated pathways in eq 1; that is, the ΔE_{LF} gap is sufficiently low that its contribution is not negligible.

The derived kinetic parameters given in Table 1 for a related series of complexes are internally consistent in the sense that only the two complexes having ΔE_{LF} gaps of between 4300 and 4600 cm^{-1} decay through both thermally activated pathways, whereas the decay curve of the complex with a low lying LF state (i.e., $Ru(bpy)_3^{2+}$) is dominated by thermal population of this state. Considering the fact that the ΔE_{LF} gap for the heteroleptic $Ru(bpy)_2(bpdz)^{2+}$ complex is expected to be larger than that of the homoleptic tris-bpdz complex owing to the stronger donor strength of the two bpy spectator ligands, relative to what would be expected with two bpdz spectator ligands, it is not surprising that the points for this complex are well modeled by ignoring a contribution from this pathway.

Conclusions

The thorough spectroscopic and photophysical characterization of the bpdz complexes studied here have identified the excited-state frequencies of the bpdz portion in both homoleptic and heteroleptic Ru complexes of bpdz. As has been observed in previous studies, the excited-state electron resides on the ligand with the lowest π^* state. In this case, that is the bpdz ligand.

Luminescence measurements revealed that the lifetime of the bpdz ^{3}MLCT state is decreased by at least a factor of 10 when the complex contains the bpy ligand.

Acknowledgment. This work was supported by a grant from the Division of Chemical Science, U.S. Department of Energy (Grant DE-FG-02-86ER13619 to J.R.K.) and the Polish State Committee for Scientific Research(Grant 3 TO9 C 01018).

References and Notes

(1) (a) Meyer, T. J. *Acc. Chem. Res.* **1978**, *11*, 94. (b) Meyer, T. J. *Acc. Chem. Res*. **1989**, *22*, 163

(2) (a) Kalyanasundaran, K., Grätzel, M., Eds.; In *Photosensitization and Photocatalysis Using Inorganic and Organometallic Compounds*; Kluwer Academic Publisher: Dordrecht, 1993. (b) Grätzel, M. *Acc. Chem. Res.* **1981**, *14*, 376. (c) Kalyanasundaran, K.; Grätzel, M. *Coord. Chem. Rev*. **1998**, *77*, 347.

(3) Kavarnos, G. J.; Turro, N. J. *Chem. Rev.* **1986**, *86*, 401

(4) Balzani, V.; Scandola, F.; In *Energy Resources Through Photochemistry and Catalysis*; Grätzel, M., Ed.; Academic Press: New York, 1983; Chapter I.

(5) Bard, A. J.; Fox, M. A. *Acc. Chem. Res.* **1995**, *28*, 141.

(6) Juris, A.; Balzani, V.; Barigelletti, F.; Compagna, S.; Belzer, P.; Zelewsky, A. v. *Coord. Chem. Rev.* **1988**, *84*, 85.

(7) (a) Clark, R. J. H.; Turtle, P.; Strommen, D.; Streusand, B.; Kincaid, J. R.; Nakamoto, K. *Inorg. Chem.* **1977**, *16*, 84−89. (b) McClanahan, S. F.; Hayes, T.; Kincaid, J. R. *J. Am. Chem. Soc.* **1983**, *105*, 4486−4487. (c) McClanahan, S. F.; Kincaid, J. R. *J. Raman Spectrosc.* **1984**, *15*, 173−178. (d) McClanahan, S. F.; Dallinger, R. F.; Holler, F. J.; Kincaid, J. R. *J. Am. Chem. Soc*. **1984**, *107*, 4853. (e) Strommen, D. P.; Mallick, P. K.; Danzer, G. D.; Lumpkin, R. S.; Kincaid, J. R. *J. Phys. Chem.* **1990**, *94*, 1357−1366. (f) Mallick, P. K.; Strommen, D. P.; Kincaid, J. R. *J. Am. Chem. Soc.* **1990**, *112*, 1686−1690. (g) Danzer, G. D.; Kincaid, J. R. *J. Phys. Chem.* **1990**, *94*, 3976−1380. (h) Danzer, G. D.; Bajdor, K.; Kincaid, J. R. *J. Raman Spectrosc.* **1993**, *24*, 357−361. (i) Ma'nuel, D. J.; Strommen, D. P.; Bhuiyan, A.; Sykora, M.; Kincaid, J. R. *J. Raman Spectrosc.* **1997**, *28*, 933−938.

(8) (a) Bradley, P. G.; Kress, N.; Hornberger, B. A.; Dallinger, R. F.; Woodruff, W. H. *J Am. Chem. Soc*. **1981**, *103*, 7441. (b) Dallinger, R. F.; Woodruff, W. H. *J. Am. Chem. Soc.* **1979**, *101*, 1355.

(9) (a) Mabrouk, P. A.; Wrighton, M. S. *Inorg. Chem.* **1986**, *25*, 526. (b) Chung, Y. C.; Leventis, N.; Wagner, P. S.; Leroi, G. E. *J. Am. Chem. Soc*. **1985**, *107*, 1416.

(10) Schoonover, J. R.; Bignossi, C. A.; Meyer, T. J. *Coord. Chem. Rev*. **1997**, *165*, 239.

(11) (a) Danzer, G. D.; Golus, J. A.; Kincaid, J. R. *J. Am. Chem. Soc*. **1993**, *115*, 8643−8648. (b) Treffert-Ziemelis, S.; Golus, J. A.; Strommen, D. P.; Kincaid, J. R. *Inorg. Chem.* **1993**, *32*, 3890−3894. (c) Treffert-Ziemelis, S.; Kincaid, J. R. *J. Raman Spectrosc.* **1994**, *25*, 893−397.

(12) (a) Schoonover, J. R.; Chen, R.; Bates, W. D.; Dyer, R. B.; Meyer, T. J. *Inorg. Chem*. **1994**, *33*, 793. (b) Schoonover, J. R.; Strouse, C. F.; Chen, R.; Bates, W. D.; Meyer, T. J. *Inorg. Chem.* **1993**, *32*, 2618.

(13) (a) Ernst, S.; Kaim, W. *Angew. Chem., Int. Ed. Engl*. **1985**, *24*, 430. (b) Ernst, S.; Kaim, W. *Inorg. Chem*. **1989**, *28*, 1520.

(14) (a) Sykora, M.; Maruszewski, K.; Treffert-Ziemelis, S. M.; Kincaid, J. R. *J. Am. Chem. Soc*. **1998**, *120*, 3490. (b) Sykora, M.; Kincaid, J. R. *Nature* **1997**, *387*, 162. (c) Sykora, M.; Kincaid, J. R.; Dutta, P. K.; Castagnola, N. B. *J. Phys. Chem*. **1999**, *103*, 309. (d) Szulbinski, W. S.; Ma'nual, D. J.; Kincaid, J. R. *Inorg. Chem*. **2001**, *40*, 3443. (e) Kincaid, J. R. *Chem. Eur. J.* **2000**, *6*, 4055. (f) Bhuiyan, A. A.; Kincaid, J. R. *Inorg. Chem.* **2001**, *40*, 4464.

(15) Lafferty, J. J.; Case, F. H. *J. Org. Chem. Soc.* **1967**, *32*, 1591.

(16) Crutchley, R. J.; Lever, A. B. P. *Inorg. Chem.* **1982**, *21*, 2276.

(17) (a) Rillema, D. P.; Blanton, C. B.; Shaver, R. J.; Jackman, D. C.; Boljadi, M.; Bundy, S.; Worl, L. A.; Meyer, T. *J. Inorg. Chem*. **1992**, *31*, 1600. (b) Meyer, T. J. *Pure Appl. Chem*. **1986**, *58*, 1193. (c) Allen, G. H.; White, R. P.; Rillema, D. P.; Meyer, T. J. *J. Am. Chem. Soc.* **1984**, *106*, 2613. (d) Lumpkin, R. S.; Kober, M. E.; Worl, L. A.; Murtaza, Z.; Meyer, T. J. *J. Phys. Chem.* **1990**, *94*, 239. (e) Rillema, D. P.; Blanton, C. B.; Shaer, R. J.; Jackman, D. C.; Boldaji, M.; Bundy, S.; Worl, L. A.; Meyer, T. J. *Inorg. Chem*. **1992**, *31*, 1600. (f) Caspar, J. V.; Meyer, T. J. *Inorg. Chem*. **1983**, *22*, 2444.

(18) (a) Danzer, G. D.; Golus, J. A.; Kincaid, J. R. *J. Am. Chem. Soc.* **1993**, *115*, 8643. (b) Danzer, G. D.; Kincaid, J. R. *J. Phys. Chem.* **1990**, *94*, 3976.

(19) (a) Maruszewski, K.; Strommen, D. P.; Handrich, K.; Kincaid, J. R. *J. Am. Chem. Soc*. **1993**, *115*, 8345. (b) Maruszewski, K.; Kincaid, J. R. *Inorg. Chem*. **1995**, *34*, 2002. (c) Szulbinski, W. S.; Kincaid, J. R. *Inorg. Chem*. **1998**, *37*, 859. (d) Sykora, M.; Kincaid, J. R. *Inorg. Chem.* **1995**, *34*, 5852.